Oscillatory rheology of aqueous foams: surfactant, liquid fraction, experimental protocol and aging effects

S. Marze,†[a] R. M. Guillermic[b] and A. Saint-Jalmes[b]

Received 6th October 2008, Accepted 9th February 2009
First published as an Advance Article on the web 23rd March 2009
DOI: 10.1039/b817543h

We report a new set of rheological data on well controlled aqueous foams. We investigate and analyze how the linear viscoelastic regime, the foam yielding and the non-linear regimes above yielding actually depends on the interfacial properties, bubble size, liquid fraction and foam age. Results are compared to previous works on foams and emulsions, and to models. The viscoelastic linear properties and yield stress are strongly dependent on the liquid fraction, and for a low molecular weight surfactant, providing "fluid-like" interfaces, a universal behavior is recovered. However, discrepancies are observed for protein foams, and are discussed in relation to the interface and thin film properties. We also discuss the features of the non linear regimes above the yield stress, which cannot be fully explained by recent models. As the foam ages, the evolution of the viscoelastic properties can be interpreted in terms of foam drainage and coarsening; nevertheless, some of the aging effects remain unexplained. We also present the results of a new mode of oscillatory experiments, at constant shear rate the macroscopic results obtained with this new protocol turn out to be strikingly well correlated to microscopic measurements at the bubble scale. We then show that a same solid-liquid transition is obtained either by applying a deformation, or by the foam coarsening; we propose that the transition is controlled by a Deborah number *De*, which can be seen either as a frequency ratio or a deformation ratio. For $De < 1$, the foam is fluid-like and the bubbles are unjammed (and the opposite is true when $De > 1$).

1. Introduction

An aqueous foam is a dispersion of a gas into a liquid, stabilized by the presence of surfactant molecules adsorbed on the gas-liquid interfaces. Depending on the relative proportions of gas and liquid, the material has various mechanical behaviors, ranging from the ones of an elastic solid to those of a viscous liquid. Foam rheology is a very active field, as illustrated in a recent review:[1] firstly, for fundamental reasons as foams are often considered as a model system for soft materials, and secondly because of the numerous industrial applications where foams are used in dynamical conditions and under flow.

Many rheological results have already been reported for 3D macroscopic foams, obtained under different modes of mechanical solicitations and with different experimental geometries.[1–11] Despite this amount of results, there are still many issues and unsolved questions. The reasons for this lack of definitive understanding are most likely due to the foam sample itself. Firstly, aqueous foams with controlled and reproducible properties are not easy to produce, especially in terms of bubble diameter D, liquid volume fraction ε, and of uniformity (meaning no initial gradients, holes, *etc*). Secondly, they irreversibly evolve in time: foams are subjected to drainage and coarsening which modify both the liquid fraction and the bubble size and create spatial and time-dependant gradients of these quantities. Lastly, foams—only a few tens of bubbles in thickness—are opaque and light is multiply scattered through them:[12,13] this prevents any simple and direct observation of the flow field inside the foam.

To avoid this latter problem, 2D foams (single layer of bubble) have been used: here, all the bubbles are always visible, as well as their deformation or velocity. In that respect, mechanical properties of such 2D foams have been widely studied both experimentally and theoretically.[14–17] 2D foams have provided some insights into the rheology of 3D samples; however, for many aspects of rheology, the specificity of the 2D experimental setup provides results which cannot be transposed to 3D. Thus 2D foams appear as rather specific systems, and cannot help to solve all the foam rheology issues.[16]

Regarding the open questions for 3D foams, it is still, for instance, not clear how the viscoelastic properties depend on the chemical formulation (surfactants, mixtures with polymers, *etc*). Authors report experimental results for very few surfactant systems.[8–11,18] Hence, the chemical aspects are still not fully explored. One can wonder if the scaling with the Laplace pressure for the elastic modulus, as often reported,[1,2,6,18] is valid for any systems, meaning that all the chemistry is included in the surface tension. Also, one can wonder about the role of the gas properties.[1] Similarly, the dependence of the viscoelastic moduli on the foam liquid fraction ε remains rather poorly measured and interpreted; here also, some data are reported but there is no full understanding of the forms of the ε-dependence.[2–6] One also has to determine and understand the complete shape of the viscoelastic elastic and loss moduli (G' and G'') while the frequency or the amplitude of the mechanical solicitation is varied, especially the non-linear regimes

[a]*Laboratoire de Physique des Solides, Université Paris-Sud, CNRS UMR 8502, Orsay, France*
[b]*Institut de Physique de Rennes, Université Rennes 1, CNRS UMR 6521, Rennes, France*
† Present address: Nestlé Research Center, Vers-chez-les-Blanc, PO Box 44, CH-1000 Lausanne 26, Switzerland.

This journal is © The Royal Society of Chemistry 2009

which are expected in the high strain and in the low frequency ranges.[19,20] In addition, the effects of aging and of slip at surfaces remain to be fully elucidated, especially as many measurements on foams need long experimental times.[1,7–9] Finally, it is interesting to determine which are the minimal parameters, at which scales, needed to describe foam rheology and how far the mechanisms revealed by foam rheology are valid for other soft systems. This non-exhaustive list of unsolved questions shows how far we still are from a full understanding of foam rheology.

The main goal of this article is first to present a full new set of rheometrical data, strongly supplementing previous results[6,18] because of better controlled experimental conditions. In particular, the dynamics of aging is better controlled by using a fluorinated gas having a low diffusivity. The various experimental improvements allow us to correctly study large ranges of bubble sizes, liquid fractions as well as different chemicals. We then present results on linear viscoelasticity, yielding, occurrence of non-linearity, and how those regimes depend on the liquid fraction, the surfactants, aging, bubble size and polydispersity. Finally, we also show the effect of the oscillation protocol: we present results obtained by oscillatory sweep at constant shear rate, rather than the usual sweeps at constant strain or frequency. Another aim of this article is to compare all these new results to the latest predictions and models.

In the following, we first describe the chemicals, the foam production methods and rheometrical apparatus in section 2, the results are then described in sections 3 and 4. In these parts, we present the data and *how* the relevant mechanical quantities change with the liquid fraction, time, chemical systems, *etc*. The discussion and analysis of all these results, explaining *why* such behaviors are found, is given in section 5 (with comparisons to previous works and available models).

2. Materials and methods

Three foaming chemicals are used: sodium dodecyl sulfate, SDS, an anionic surfactant; a milk protein, casein (CAS); and Amilite GCK-12 (GCK), an amino-acid based surfactant kindly provided by Ajinomoto co., inc. For the SDS and CAS solutions, the concentrations used are $c_{SDS} = 6$ g L^{-1} and $c_{CAS} = 4.5$ g L^{-1}. The later is brought at pH 5.6 by adding a phosphate buffer at 10 mM, and then placed in an ultrasonic bath for 30 min, so as to prevent casein from aggregating during the dissolution. The solution is then stirred at 1000 rpm for 8 hours. After this procedure, the CAS solution can be used for two days before any bacteria development. For GCK, the solution pH is 8.2 with a concentration of $c_{GCK} = 10$ g L^{-1} in neutral water (no buffer is needed at room temperature). The gas used is C_2F_6, which has low diffusion and solubility constants, considerably limiting coarsening and drainage of the foams, as also discussed in.[18,21] All the experiments are performed at 20 ± 2 °C.

For each solution, the surface tension is measured by the rising bubble shape method. An equilibrium value is reached within a minute after the formation of the bubble for SDS and GCK. For CAS, after a fast decay, there is no equilibrium; a slow continuous decrease (of a couple of mN/m) is still observed with time. We use the value at a typical instant of 300 s corresponding to the mean duration of a rheological measurement. The surface tensions σ are 36, 22 and 46 ($\pm$0.5) mN m^{-1} for SDS, GCK and CAS respectively. Note that surfactant solutions all have the same Newtonian viscosity $\mu = 1 \times 10^{-3}$ Pa s, as determined in a double-gap cylindrical Couette geometry.

We use two methods to produce aqueous foams: first, a turbulent mixer apparatus described in,[22] and secondly, a bubbling method consisting of blowing gas into porous glass frits (with various porosities) immersed in the surfactant solution. Both techniques give complementary foams: the first one produces slightly polydisperse foams with sub-millimetric bubbles and liquid volume fraction varying from 0.05 up to 0.25 in this study;[22] while the second method produces more monodisperse foams with millimetric bubbles and liquid volume fraction ranges from 0.01 up to 0.06 in this work. The liquid volume fractions of the samples are measured by electrical conductivity.[23] The bubble mean radius R is measured at the surface of fresh foams samples by optical microscopy. For each type of foam, 10 samples are imaged. The mean value is calculated from all those measurements. For SDS, GCK and CAS foams produced with the turbulent mixer apparatus, $R = 60 \pm 5$ μm. For SDS and CAS foams, three bubble radii are obtained with the bubbling method, each associated to a liquid volume fraction value: $R = 1.13$ mm at $\varepsilon = 0.01$; $R = 0.52$ mm at $\varepsilon = 0.03$; $R = 0.19$ mm at $\varepsilon = 0.06$.

We have also used the thin film balance apparatus to separately study single film films:[24] as already reported, thin flat and uniform films are obtained for SDS and GCK (with film thickness h equal to 30–40 nm), while thick and gelified films are found for CAS[18,25] (thickness is not homogeneous, and varies between 200 and 300 nm). Note that if the thin films separating the bubbles are similar for SDS and GCK solutions, the interfacial viscoelastic properties in compression are different. GCK interfaces have higher elastic and viscous interfacial moduli in compression: the elastic modulus $E' = 12$ mN m^{-1} and the viscous one, $E'' = 47$ mN m^{-1}; for SDS, we get $E' \approx E'' \approx 1$–2 mN m^{-1}. The CAS interface have also different viscoelastic properties with $E' = 15$ mN m^{-1} and $E'' = 8$ mN m^{-1}. All these measurements are performed at a frequency of 0.2 Hz. Thus, by using the three chemical systems, we can expect that both interfaces and films properties are significantly varied.

The rheometer is a commercial MCR 300 from Paar Physica. Two home-made geometries are used: "cone-plate" and "plate-plate" systems, made in Plexiglas, and both having a diameter of $d_0 = 175$ mm. To avoid wall slip, cone and plates are covered by polydisperse sand grains with a mean diameter around 100 μm. The cone angle is 10°. We focus here on oscillations modes, steady-shear with and without slip is described in another article.[9]

3. Results of strain-sweep tests: oscillations at constant frequency and variable strains

3.1 Definitions and qualitative description of the stress and moduli curves

Typical results of strain-sweeps for SDS foams at a fixed liquid volume fraction are displayed in Fig. 1. This sweep procedure consists in the application of a strain γ varying from 0.005 up to 5, at a constant frequency $f = 1$ Hz. The storage G' and the loss

 This journal is © The Royal Society of Chemistry 2009

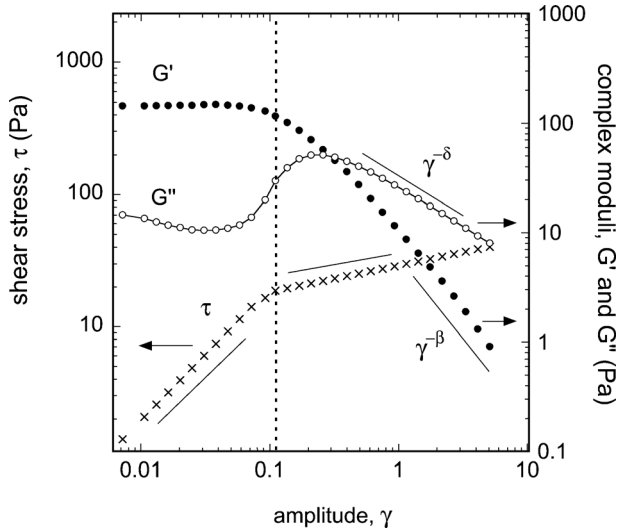

Fig. 1 Typical results for strain-sweep oscillations (SDS foams $\varepsilon = 0.15$). The stress τ, G' and G'' are plotted as a function of the strain γ. Linear regime, yielding features and non-linear parts are well evidenced. The vertical dashed line shows the position of the yield strain γ_y: for lower strains, the linear regime is obtained and $\tau \approx \gamma$; while above γ_y, $\tau \approx \gamma^{\alpha}$ with $\alpha < 1$.

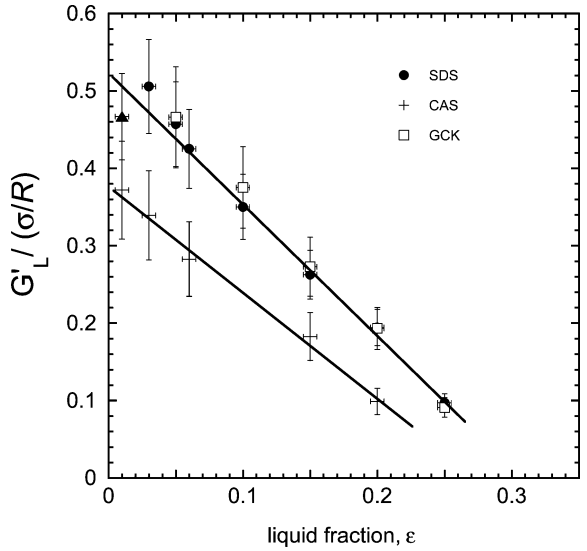

Fig. 2 Dependence of the elastic modulus G'_L (measured in the linear regime) on the liquid fraction for the different bubble radii and chemical systems. The modulus is normalized by the Laplace pressure (σ/R). For all the chemical systems, $R = 1.13$ mm for $\varepsilon = 0.01$, $R = 0.52$ mm for $\varepsilon = 0.03$, $R = 0.19$ mm and 0.06 mm for $\varepsilon = 0.06$ while the bubble diameter is $R = 0.06$ mm for all the other liquid fractions. The solid lines correspond to the asymptotic regime of the eqn 2 in the limit of low ε, as discussed in the text.

G'' moduli are classically obtained from those measurements, as well as the shear stress τ.

We first describe how the stress and the viscoelastic moduli qualitatively depend on γ, allowing us to introduce some definitions. The shear stress shows two well-defined regimes: a linear regime $\tau \approx \gamma$ at small strain strains followed by second regime where $\tau \approx \gamma^{\alpha}$, with $\alpha < 1$, at larger strains. The kink between those regimes defines the yield point: γ_y and τ_y.

For the elastic modulus, a plateau (at $G' = G'_L$) is observed at small strains, consistent with the linear behavior of the stress. Well above the yield strain, G' decreases with a power law $G' = G'_{NL}\,\gamma^{-\beta}$.

The loss modulus has a more complicated dependence on the strain γ. At low γ, and down to the usual smallest strains, a value almost independent of the strain is found (G''_L), as for G'. Note that G'' is less constant that G' in that range, and it is often observed that it slightly decreases with γ. At higher strain, the G'' profile shows a large bump, then it finally decreases with a power law $G'' = G''_{NL}\,\gamma^{-\delta}$. As γ increases, the G' and G'' curves cross each other, after the yield point. These qualitative descriptions remain valid for all the liquid fractions, and all surfactant systems. As the liquid fraction is varied, all the curves are shifted vertically (decreasing ε shift the curves downward and the yield stress and strain decrease), but the global shapes remain similar. This means that all the quantities defined before, below and above yielding, can always be measured. Their quantitative variations are presented in the next section.

3.2 Quantitative variations with the foam parameters

We first describe how the change of surfactant, liquid fraction and foam age quantitatively modify the results for the linear regime (meaning $\tau \approx \gamma$ and a constant G'_L). As initially pointed out by Derjaguin,[26] the characteristic scale for the elastic modulus G'_L is the Laplace pressure, σ/R, and many results have confirmed this scaling.[1,6] In Fig. 2, the measurements for different bubble radii and surfactant systems of G'_L normalized by σ/R are compiled and plotted as a function of the liquid fraction ε. Qualitatively, one recovers that the foam becomes less elastic as the liquid fraction increases, since the bubbles are less and less packed. All the normalized measurements with SDS and GCK, whatever the bubble radii, collapse on a single curve. On the contrary, the values for CAS are always lower. These results will be analyzed in section 5.

Similarly, the Fig. 3a shows how G''_L, normalized by (σ/R), varies with the liquid fraction. Here again, there are no differences between SDS and GCK, at all the liquid fractions. The CAS foams give different results: on the contrary of Fig. 2, the values are now found to be higher than with SDS and GCK.

In Fig. 4a, we show how the moduli evolve with time, for two surfactant systems. The strain and frequency are kept constant ($\gamma = 0.005$, and $f = 1$ Hz) and we monitor G' and G''. Clearly, the aging behavior depends on the interfacial properties; in particular, a strong decreases of G'' is found for the SDS foams and not for the CAS ones. Another way to evidence the aging effect is shown in Fig. 4b. Here for a the starting time t_0, the strain-sweep measurement is started at two initial values of strain γ_0 ($\gamma_0 = 0.005$ and $\gamma_0 = 0.05$). The measurement curve is obtained point by point by increasing values of the amplitude. Thus, by changing γ_0, the measurements at a given $\gamma > \gamma_0$ are made at different foam ages. Following this protocol, we recover the aging effect for the SDS foam seen in Fig. 4a. Note that if we take only the values measured at short times on the fresh foams, G''_L appears independent of the strain γ. Secondly, one can also see that the differences vanish at high γ. In agreement with Fig. 4a,

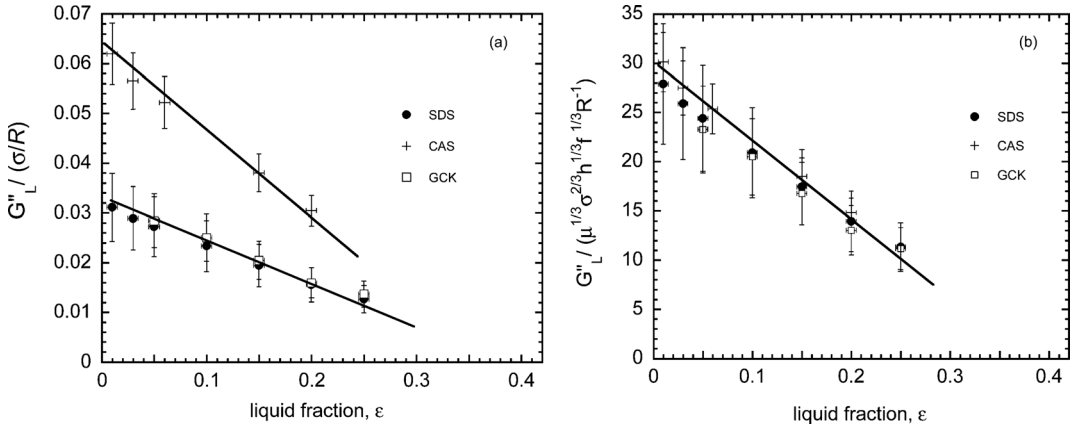

Fig. 3 Dependence of the loss modulus G''_L (measured in the linear regime) on the liquid fraction for the different bubble radii and chemical systems. (a) The modulus is simply normalized by the Laplace pressure σ/R; (b) another normalization is tested, including viscosity and film thickness. Bubble radii are the same as in Fig. 2: for all the chemical systems, $R = 1.13$ mm for $\varepsilon = 0.01$, $R = 0.52$ mm for $\varepsilon = 0.03$, $R = 0.19$ mm and 0.06 mm for $\varepsilon = 0.06$ while the bubble diameter is $R = 0.06$ mm for all the other liquid fractions.

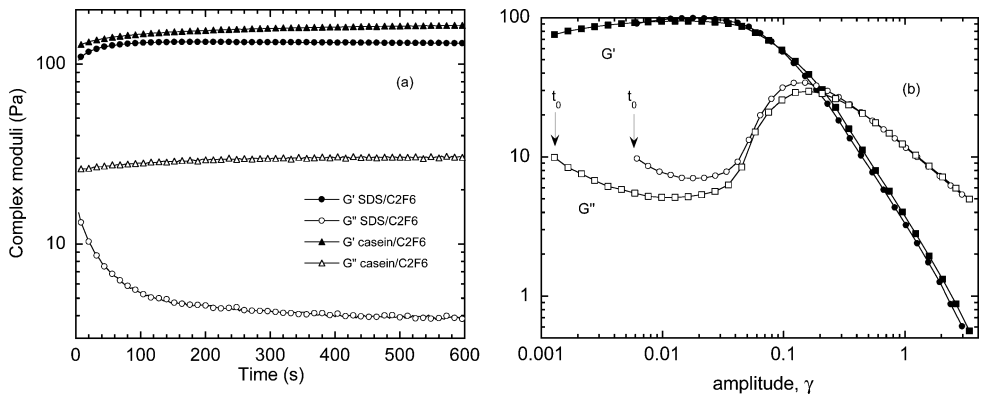

Fig. 4 (a) Measurements as a function of time of the elastic and loss moduli for SDS and CAS foams ($R = 60$ μm), made with C_2F_6. (b) Strain-sweep experiments started at time t_0 with different initial amplitude value γ_0, also evidencing the aging effects.

the same time test for a CAS foam shows a quasi-constant G''_L. In creep tests, those time effects are also visible if one starts the measurement at different foam ages (different waiting times t_w from the foam production). After an initial elastic strain jump, the curvature of the creep stage indeed depends more on waiting time for SDS foams than for CAS ones.[18,25]

In Fig. 5, we have plotted the volume fraction dependence of the yield stress τ_y normalized by the Laplace pressure. Compared to the G' and G'' data, those on τ_y appears more noisy. In that respect, apart some values slightly a bit lower for the CAS foams, no clear effects of the surfactant are observed. For the driest foams, the data are the most spread, mostly those for the most monodisperse foams produced by the bubbling method. Nevertheless, we have not found systematic deviations with polydispersity. Note that we have also add the measurement obtained by applying a continuous shear rate $\dot{\gamma}$, and by extrapolating the stress in the limit of zero $\dot{\gamma}$ (open symbols in Fig. 5). Once again, through the noise, some relative agreement between the two approaches is observed, which seems less and less valid as the liquid fraction increases.

Above the yield point, as shown in Fig. 1, power laws for G' and G'' are observed at large strains: the exponent β is 1.42 ±

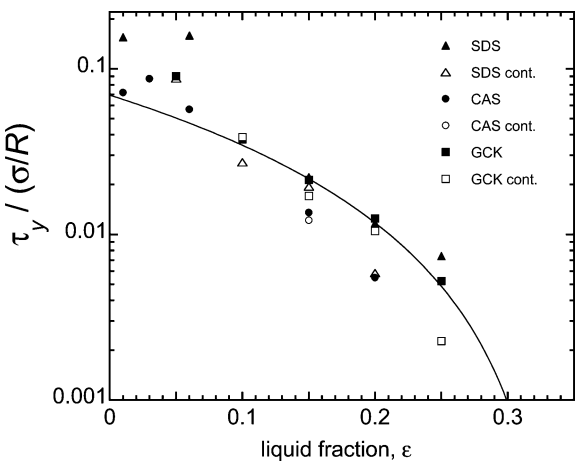

Fig. 5 Yield stress *vs* liquid fraction, for various bubble radii and chemical systems. Results are obtained either by oscillations (full symbols) or from steady-shear data (empty symbols). The solid line is a fit following eqn 4. Bubble radii are the same as in Fig. 2: for all the chemical systems, $R = 1.13$ mm for $\varepsilon = 0.01$, $R = 0.52$ mm for $\varepsilon = 0.03$, $R = 0.19$ mm and 0.06 mm for $\varepsilon = 0.06$ while the bubble diameter is $R = 0.06$ mm for all the other liquid fractions.

This journal is © The Royal Society of Chemistry 2009

0.02, and does not depend on the liquid volume fraction down to $\varepsilon = 0.03$ where it becomes 1.49. For $\varepsilon = 0.01$, the foam is too fragile and breaks in the beginning of the nonlinear regime. For G'', the exponent δ depends more on the liquid volume fraction, from 0.66 to 0.85 when ε is changed from 0.25 to 0.03. Note that it also depends more on the surfactant systems, varying from 0.7 to 0.85 from SDS foams to CAS ones. Lastly, concerning the stress dependence with γ, above yielding, a power law is observed and its exponent increases with frequency f and with the liquid fraction, as already observed in.[6]

4. Results of oscillations at constant shear rate: varying simultaneously strain and frequency

Together with strain-sweeps, one usually performs frequency-sweep experiments: the oscillation is made at various frequency f, while the strain γ is kept constant. Such measurements have already been reported for foams:[5,6] an almost constant value is found for G' and G'' for a large range of frequencies, typically 10^{-2} Hz < f < 10 Hz. As well, non-linear effects occur at the highest frequencies (f > 10 Hz), interpreted in terms of "weak planes".[27] On the opposite limit, it has been shown that the low frequency behavior is strongly coupled to the foam coarsening, which is eventually able to relax the stresses and to unjam the foam. The foam is expected to recover a liquid-like behavior with G'' > G'.[1,7] Creep tests have shown that a viscous flow is always observed at long times with the viscosity depending on the gas used.[1,18] However, all the features of the low frequency behavior are not understood, especially because it requires long measurement times ($t_{exp} \approx 1/f$) meaning that all aging processes induce drastic foam changes during any single measurement.

Recently, it has been suggested that the classical frequency-sweep protocol might not be the only and most relevant way to probe the properties of such soft materials. Another procedure consists of varying γ and $\omega = 2\pi f$ simultaneously and inversely, so that their product, defining a shear rate $\dot{\gamma} = \gamma\omega$, remains constant.[28,29] Note that in a previous work, we showed that some agreement between oscillatory shear and steady shear is found when the above definition of the oscillatory shear rate is used (with the angular frequency).[9] The motivation for doing this experimental protocol comes from the observation that the rate of the slow relaxation process often depends solely on the shear rate, rather than on other quantities. In that respect, the usual frequency-sweep is not ideal: the shear rate changes from one point to another. We have performed such new oscillatory experiments *at constant shear rate* on our home-made GCK and SDS foams, at a fixed given liquid fraction. The results for two constant shear rate ($\dot{\gamma}_1$ and $\dot{\gamma}_2$) are plotted in Fig. 6a and 6b. When the results are plotted as a function of the angular frequency, we observe a profile with a bump in G'', associated to a kink in G', and power law scaling at the lowest frequencies. The curves are completely different from the usual flat region observed at these frequencies when γ is kept constant. In fact, it looks exactly like the shape expected in the limit of zero frequency: G'' becoming bigger than G' at low ω. Secondly, it is found that, from one shear rate to the other, the same curves are simply shifted towards higher values of frequency. On the contrary, there is almost no shift in the vertical axis. At all shear rates, some power laws at low frequencies are observed $G' \approx \omega^{\beta'}$ and $G'' \approx \omega^{\delta'}$.

Now, if the results are plotted *vs* the strain γ, we observed no effect with the shear rate: all the curves collapse. Moreover, the curves collapse precisely on the curve of the strain-sweep performed at constant frequency (Fig. 6b). Thus, performing a strain-sweep at any fixed shear rate or at a fixed frequency provides the same results.

To get more information, we have studied Gillette shaving foams, in order to compare our data to other published results. Qualitatively, the same behaviors are observed. The collapse of the curve as a function of the amplitude is less valid for the smallest shear rates we tested. In this limit of low shear rate, we also observe that there is less and less variations of the results when plotted as a function of frequency; in fact, the results seem to tend to a constant curve independent of the shear rate. But it is difficult to performed valid measurements in these limits of low shear rates, as the interesting features of the curves (bump in G'')

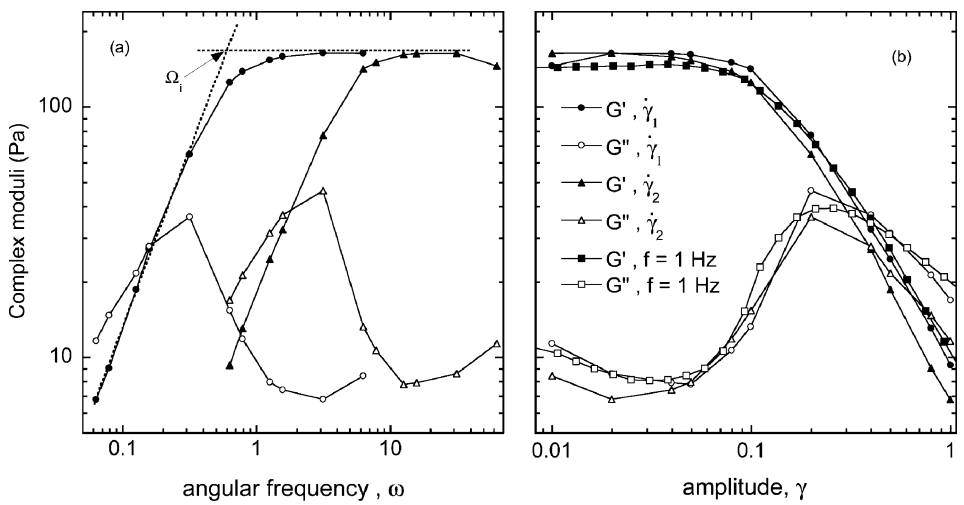

Fig. 6 Elastic and viscous moduli, G' (full symbols) and G'' (open symbols), measured by oscillations *at constant shear rate*, for two values of the shear rate, $\dot{\gamma} = 0.06$ s^{-1} (circles) and $\dot{\gamma} = 0.6$ s^{-1} (triangles). (a) G' and G'' are plotted *vs* the frequency ω, and the dashed lines show how the characteristic frequency Ω_i is obtained. (b) G' and G'' are plotted *vs* the strain γ; for comparison, we also add the curve at a fixed frequency $f = 1$ Hz (squares).

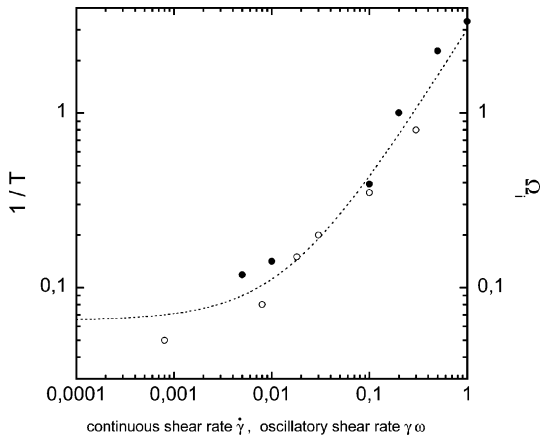

Fig. 7 Left vertical axis: bubble rearrangement rate, $1/T$ as a function of the steady shear rate $\dot{\gamma}$, measured by DWS, results from[35] (open symbols). Right vertical axis: characteristic frequency, Ω_i, corresponding to the kink in G' (as shown in Fig. 6) as a function of the oscillatory shear rate $\dot{\gamma}$ (full symbols). The dashed line represents eqn 1.

are shifted towards very low frequencies, meaning very long experimental time, and the data become more and more noisy.

Since it turns out that the curves are simply translated in frequency, the evolution of the curves with the shear rate $\dot{\gamma}$ can be represented by the way a typical frequency evolves with $\dot{\gamma}$. We have chosen to monitor the frequency Ω_i which corresponds to the kink in G', as shown in Fig. 6a. We will come back to this choice in the discussion. The evolution of Ω_i is reported in Fig. 7, and can be adjusted in the following form:

$$\Omega_i = \Omega_i^0 + \frac{1}{\gamma_c}\dot{\gamma}^{\xi} \quad (1)$$

The best exponent ξ is found to be slightly below 1. However, note that we do not have enough accuracy to precisely determine the limit $\Omega_i^{\,o}$ at the limit of zero $\dot{\gamma}$. In Fig. 8, we show another way

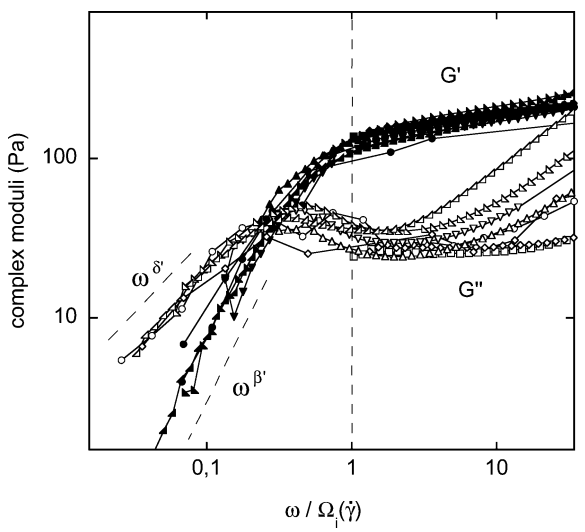

Fig. 8 Elastic and viscous moduli G' and G'' as a function of the re-scaled frequency ω/Ω_i: expect at the highest frequency, all the curves collapse, and the kink in G' is localized at $\omega/\Omega_i = 1$ (vertical dashed line). For $\omega/\Omega_i > 1$, a solid-like behavior is found, and the opposite is true when $\omega/\Omega_i < 1$.

to view these results: all the curves can be collapsed on a master curve, when the experimental frequency is normalized by the function $\Omega_i(\dot{\gamma})$. In this graph, it is quite clear that the power law exponents at low ω for G' and G'', β' and δ', appears independent of $\dot{\gamma}$. More strikingly, these parameters are quite close to the exponent at high strains, $\beta' \approx \beta$ and $\delta' \approx \delta$. Note that at the limit of high ω, the collapse of the curve is not seen, showing that this normalisation by the shear rate is not relevant for the non-linear effects seen at high ω.[27]

5. Discussion

5.1 The linear regime: variation of G'_L and G''_L

These results clearly show that there is an effect of the molecules adsorbed on the viscoelastic moduli in the linear regime. This is consistent with our previous work only at $\varepsilon = 0.15$,[18] and also with previous results on steady-shear.[8–11] In fact, the analysis of these results and the comparisons to others tend to show that it is the CAS foams which have an unusual behavior, while SDS and GCK foams have a standard one.

Let first analyze the results for SDS and GCK. Once normalized by the Laplace pressure, the moduli are indeed quite consistent with previous works both on foams and on emulsions, done at very different bubbles or droplets sizes.[6,30–32] The limit at $\varepsilon = 0$, where $G'_L/(\sigma/R) \approx 0.52 \pm 0.02$, and the dependence of G'_L with ε are quantitatively identical, and in agreement with predictions.[6,33] Concerning this dependence on ε, some phenomenon-based laws have been proposed,[30] stating that:

$$G'_L/(\sigma/R) \approx (1-\varepsilon)(\varepsilon_c - \varepsilon) \quad (2)$$

Our data can actually be adjusted by this model, and we consistently find that ε_c is close to 0.34 ± 0.02. In the limit of dry foams, the law is approximately in $(\varepsilon_c - \varepsilon)$, as shown by straight lines in Fig. 2. In addition, polydispersity, which here remains relatively low and is not widely varied, is not modifying these standard results.

For G''_L, SDS and GCK data can also be collapsed by a similar scaling with the Laplace pressure, as also found for emulsions.[30–32] Note that, though the Laplace pressure is a natural scale for the elasticity,[26] it is not at all obvious to state that it is also the right scale for G''_L. In addition, for $G''_L/(\sigma/R)$ at the limit of $\varepsilon = 0$, there are no predictions; our normalized results are consistent with previous ones for foams, but compared to those for emulsions[30–32] they are about 5 times higher. This difference remains to be understood, and all together, it seems to us that the understanding of the dissipative part, in the linear regime at low γ, is still far from complete.

We then have to find out what the origins of the behavior of the CAS foams are. We are tempted to consider that the unusual behavior of G'_L should probably not be decoupled from the unusual behavior of G''_L: the reason for the high values of G''_L and the low values of G'_L is probably the same. As already introduced, the main differences between the SDS/GCK foams and the CAS ones are: (i) SDS and GCK molecules are small molecular weight surfactants (meaning fast dynamics at the interface and in exchange with the bulk), while CAS molecules are large and slow proteins, attached irreversibly to the interface (at least, when compared to the others); (ii) these differences

 This journal is © The Royal Society of Chemistry 2009

induce different surface viscoelastic behavior, as described previously; (iii) the films between the bubbles are thin and flat for SDS and GCK, while they are thick and appear gelified for CAS; and (iv) the aging (drainage and coarsening) of these foams are also different (we will come back to this point in section 5.2). At this stage, we can only speculate, though it seems quite plausible, that there are links between the thin film texture and thickness and the higher values of G''_L, which means higher dissipation. But this does not provide any reasons for the lower G'_L. It is also possible that side effects, like slip at the rheometer plate surface, come into play for CAS foams more than for the others.

Note also that the SDS and GCK foams looks very similar, despite some known differences in their interfacial rheological behavior: this could mean that purely interfacial properties may not be relevant and that all the low molecular weight surfactants (making flat and thin liquid films) are identical. However, the lack of difference seen here may also be due to the fact that the two systems are not different enough in terms of interfacial viscoelasticity. Experiments with mixture of surfactant and insoluble fatty acid salts, providing compression viscoelastic moduli of about a few hundreds of mM m^{-1}, have evidenced some effects of these interfacial properties.[10,11]

Back to the possible role of the film thickness h, it may be introduced into existing scaling laws for G''_L. Indeed, starting from the thin films energy dissipation over a sinusoidal extensional strain cycle on 2D dry foams or emulsions, Schwartz and Princen,[34] followed by Reinelt and Kraynik,[35] came to the result:

$$G''_L = C\frac{\mu^x \sigma^{1-x} h^y f^x \gamma^w}{R^z} \quad (3)$$

with the dimensional condition $z - y = 1 - x$, and C being a numerical factor. In both references $x = 2/3$ and $y = 0$, but for w and C, the results are different.

We find that it is possible to rescale all our data by adding this film thickness effect with $x = 1/3$, $y = 1/3$ and $w = 0$: with this scaling, all the loss moduli G''_L at low strains can be collapsed (Fig. 3b). This implies then only a small dependence with the viscosity, which is consistent with previous published results.[18] This type of scaling thus could appear qualitatively interesting, but it is only valid for G''_L, and it cannot explain either the G'_L behavior, or the quantitative variations of G''_L with time, as discussed below.

Lastly, one can compare the relative importance of the physical (liquid fraction and bubble diameter) and chemical parameters: it is clear that if one want to tune quantitatively the viscoelastic moduli, it is much more efficient to act on the liquid fraction or on the bubble diameter, rather than by changing the adsorbed surfactants (especially as the surface tension is always within the same range of values at gas–liquid interfaces).

5.2 Aging effects

The evolutions with time, as described in Fig. 4a and b, can be analyzed in relation to the foam drainage and coarsening which both act on the liquid fraction and on the bubble size. Indeed, as seen before, G'_L and G''_L are functions of R and ε, and these quantities change with time. With C_2F_6, the coarsening is strongly slower than with air[21] and one can expect to keep the bubble size approximately constant during the experiment. However, this low coarsening rate also depends on the interfacial properties, and it is about 5–7 times faster with SDS than with CAS (interpreted in relation to the different film thickness).[18] Besides coarsening, the foams are also draining, which tends to make them drier with time. We expect that this effect is the main one occurring at shorter times. Indeed, the experimental observations are consistent with this scheme: the increase of the moduli with time can be explained by the decrease of the average ε.

In that respect, the decrease of G'' for the SDS foam is then not straightforward to understand. Surprisingly, the supposedly simplest case gives the most unexpected behavior. Back to the scaling discussed in section 5.1 (eqn 3), the decrease of G'' could be linked to the variation of the film thickness; but this would imply variations of h which are too large (about a factor of 30), and on two long time scales (minutes). There are in fact no reasons for such a long film drainage time with these bubble sizes, and the films are already quite thin at shorter times. It is most likely linked to coarsening and the rate of bubble rearrangement since these unexplained aging effects occur for SDS and not for CAS.

5.3 Yielding and non linear regimes

Previous published results have shown that the yield stress depends on the liquid fraction following:

$$\tau_y = k(\sigma/R)(\varepsilon_c - \varepsilon)^2 \quad (4)$$

Mason *et al.* found $k = 0.51$ and $\varepsilon_c = 0.37 \pm 0.01$ for emulsions.[30] This result is also found in ref. 6 for aqueous foams, with $k = 0.53$ and $\varepsilon_c = 0.365 \pm 0.01$. We have also tested this functional form as shown in Fig. 5: it turns out that our data can also be adjusted by this form, and the prefactor k is here equal to 0.62, slightly above the previous results but still in fair agreement. In fact, the data are more spread out and the accuracy of k and of ε_c is not high: nevertheless, we find that $\varepsilon_c = 0.35 \pm 0.03$. For other comparisons, theoretical developments give some insights into the very dry limit. Those are detailed in a review article by Princen.[2] So far, except for the quasi-monodisperse aqueous foam case in[36] for which the τ_y normalization limit is 0.7, all authors agree on a theoretical dry limit value of 0.15 ± 0.05.[2] Still, the spreading of the data is not well-understood. Note also that, as for G'_L, the effect of the bubble radius appears to be fully captured *via* the scaling with the Laplace pressure: $G'_L \approx \tau_y \approx R^{-1}$.

Concerning the comparisons between the yield stress extracted either from oscillatory measurements or from continuous shear rate measurements (Fig. 5), the fact that we see not much differences could mean that the shear flows are homogeneous (differences have been sometimes correlated to shear localization or banding).[31] However, our yield stress data are still probably too noisy to definitively conclude on this point.

Lastly, we can analyze the power law exponents β and δ of G' and G'' ($G' \approx \gamma^{-\beta}$, $G'' \approx \gamma^{-\delta}$). On one hand, a factor of 2 is often observed experimentally, as reported in ref. 28. In this work, Miyazaki *et al.* found $\beta = 1.8$ and $\delta = 0.9$ by measurements and simulations of dense hard-sphere colloidal suspensions.[28] Recently, experiments on sheared interfacial monolayers have shown similar exponents and behavior.[37] On the other hand,

from the theoretical point of view, Höhler *et al.*[20] and Marmottant and Graner[19] recently found with elasto-plastic models (including viscosity in ref. 19) that the exponents are $\beta = 1.5$ and $\delta = 1$. Our results are consistent with the range of expected values, but it remains hard to say if they fit a particular description. In general, our results fairly agree with ref. 28 on the factor of 2 between the exponents. In any case, a value of 1 for δ is always too large to describe our data, but at the same time the measured values for β agree with the predicted value (1.5).

5.4 The constant shear rate data

From these measurements shown in Fig. 7 and 8, it turns out that scanning the sample frequency with a constant shear rate $\dot{\gamma}$, rather than with constant strain γ, provides more information and allows the evidencing of new features, usually hidden if the sweep is simply done at fixed γ. It turns out to be a clever way of observing the low frequency behavior: the main point here is that what occurs at extremely low frequencies (under no shear) becomes observable in a more accessible frequency range, simply by applying a shear rate.

These experiments confirm that the sample has an intrinsic relaxation process with a typical internal frequency being a function of the shear rate only. Thus, when $\dot{\gamma}$ is conserved along the frequency-sweep, the internal frequency remains constant: it becomes then possible to get specific features (a bump in G'', a kink in G' and thus a cross between G' and G'') when the experimental frequency of the oscillation ω becomes similar to this internal relaxation frequency Ω_i. In that respect, in the classical frequency-sweep curves, one can understand that a featureless plateau in G'' is observed, since one continuously jumps from one measurement at a given $\dot{\gamma}$ to a measurement at another $\dot{\gamma}$.

The dependence of the relaxation process with $\dot{\gamma}$ is described by the function Ω_i (eqn 1). Two different regimes can be identified: at low shear rate, the frequency Ω_i is independent of $\dot{\gamma}$, while it is approximately linear with $\dot{\gamma}$ at higher values. The first regime corresponds to a dynamics of bubble rearrangement inside the sample controlled by the coarsening, whereas the dynamics is controlled purely by the shear at the highest $\dot{\gamma}$. The crossover between the two cases is rather smooth, as already observed with DWS data.[38] Indeed, in order to connect our macroscopic measurements to those obtained at the bubble scale, we have compared them to multiple light scattering (DWS) data.[38] With this technique, the rate of bubble rearrangement—either induced by coarsening or by applied shear—is measured. It turns out that there is a very good agreement between these microscopic measurements at the scale of the bubble size and the macroscopic ones obtained by oscillations at constant shear rate. In Fig. 7, we have added the DWS measurements from Gopal and Durian[38] (open symbols), and one can see that the inverse of the typical timescale obtained by DWS and the measured angular frequency deduced from the oscillatory measurements (full symbols) coincides well, once they are respectively plotted as a function of the steady shear rate and of the oscillatory shear rate. This confirms again that steady shear and oscillatory shear can be equivalent.[9] In the limit of zero shear rate, the frequency is controlled by coarsening, it must decrease with the foam age. Indeed, smaller frequencies (longer timescales) were found in[7] by performing long duration relaxation rheological experiments (at least at longer timescales than the measurements reported here).

When these oscillatory data are plotted as a function of the strain γ (Fig. 6b), the bump occurs for the same reasons, when the relaxation process frequency controlled by the shear rate equals the experimental oscillation frequency. Apart for the lowest shear rates, as the internal frequency Ω_i is almost linear in $\dot{\gamma}$, $\Omega_i \approx \dot{\gamma}/\gamma_c$, equating this typical frequency Ω_i to the experimental one $\omega = \dot{\gamma}/\gamma$ implies that the kink in G' (defining Ω_i) always occurs at the same fixed value of strain, $\gamma = \gamma_c$, and this remain true whatever $\dot{\gamma}$. This explains why the experimental curves are independent of the shear rate $\dot{\gamma}$or frequency when plotted as a function of the strain (Fig. 6b). Firstly, note that this is important to validate all the previous discussions (sections 5.1, 5.2 and 5.3) based on strain-sweep measurements. Secondly, we can identify the value γ_c obtained by fitting $\Omega_i(\dot{\gamma})$ to the foam yield strain γ_y: due to the choice that we have made for positioning Ω_i (at the kink in G'), it comes that—once plotted along the strain axis—this position corresponds exactly to the one defining the yield strain, as shown in Fig. 1. Thus, by construction, $\gamma_c = \gamma_y$; indeed, we extract a value of 0.25 for γ_y from the slope of $\Omega_i(\dot{\gamma})$ at high $\dot{\gamma}$ (Fig. 7), and it is completely in agreement with usual oscillation measurements.

Still in this regime dominated by shear rate, one can write:

$$\frac{\gamma_c}{\gamma} \approx \frac{\omega}{\Omega_i} = De \tag{5}$$

This ratio can actually be recognized as a Deborah number, *De*: it is the ratio between a typical intrinsic relaxation time ($t_i \approx 1/\Omega_i$) and an experimental time ($t_{exp} \approx 1/\omega$). At the kink in G', $De = 1$ ($\omega = \Omega_i$ and $\gamma = \gamma_y$). For $De < 1$, corresponding to long timescales or large deformations, the foam is fluid-like ($G' < G''$) and the bubbles are unjammed, while for $De > 1$, the foam responds elastically ($G' > G''$). This ratio thus appears as a control parameter describing the solid-liquid (or jamming) transition in a foam, either induced by coarsening or by applied shear.

We also want to make a few last remarks on these results. First we want to stress out that the same exponents are found at low frequency and high strain for G' and G'' ($\delta' \approx \delta$ and $\beta' \sim \beta$). As well, the exponent β' and δ' are independent of the shear rate. All together, this seems to us possible only if a same microscopic mechanism is involved in the stress relaxation in all these situations: at low frequency where coarsening is acting, and at high strain where shear is acting. In fact, this is the case for foams: at the bubble scale, it is known that the unjamming of the foam is always done by a single elementary process, the bubble side-swapping (known as T1). Moreover, a T1 induced by coarsening and a T1 induced by shear are topologically the same, and this is an important ingredient required for obtaining such symmetries between low frequencies and high strain non-linear regimes. Moreover, it is striking to find that the exponent ξ deduced from $F_i(\dot{\gamma})$ (eqn 1) is also quite close to δ and δ'. One can wonder if this common value of the power law exponent (found between 0.65 and 0.9, depending on the liquid fraction and the surfactant system) is really meaningful and significantly different from 1. In fact, it is also found for many different other systems,[29] always significantly smaller than 1. Thus, we believe that this value has a real physical meaning, all the more since a close exponent (0.8

 This journal is © The Royal Society of Chemistry 2009

$\pm$ 0.05) is also found for the viscosity *vs* shear rate.[7] As well, this is also in agreement with the measurements of the viscous stress as a function of the shear rate,[8,9] where exponents between 0.2 and 0.45 are found (by definition these exponents of the viscous stress are equal to $1 - \delta$). Since the viscosity is inversely proportional to the internal relaxation frequency, we understand this common exponent as a characteristic of the shear-thinning process, which is thus induced by the T1 rate increase with $\dot{\gamma}$. As both rheology and DWS probe this T1 rate, and as steady shear rate and oscillatory shear rate agree, then the three exponents should have this identical origin. Note also that the fact that ξ is smaller than 1 could come from a small dependence of the yield strain γ_c with $\dot{\gamma}$: the dependence of Ω_i with $\dot{\gamma}$ reported in eqn 1 can actually be the result of a linear function of $\dot{\gamma}$, divided by a smooth function $\gamma_c(\dot{\gamma}) = \dot{\gamma}^{\lambda}$, with $\lambda = 1 - \xi \approx 0.1$.

As already pointed out, there are lots of similarities between the results presented here and those for quite different systems (from colloidal suspensions, to hydrogels and interfacial layers);[28,29,37] all share the same features of a relaxation time which depends only on the applied shear rate, in association with yielding and shear thinning. Note lastly that concerning the origin of the bump in the G'' curve of Fig. 6a, we have seen that it occurs when the experimental frequency at which the sample is scanned corresponds to some internal relaxation frequency. Such a scheme is also proposed in relation to effective temperature in the system undergoing aging and jamming. Abou and Gallet showed that, for a solution of clay (laponite), a peak in temperature occurs when there is an accommodation between the experimental frequency and the internal frequency (which evolve with age).[39] When the sample is scanned at this frequency, the temperature is measured higher than the bath, as here where we get a maximum in G''.

6. Summary and conclusions

We have obtained a new set of data on foam linear and non-linear viscoelasticity. Our data significantly increase the experimental knowledge on foams. In particular, the effects of the surfactant molecules and of the liquid fraction have been widely investigated and analyzed.

We have found that, once G'_L is scaled by the Laplace pressure, its decrease with the liquid fraction ε is similar to the one seen for emulsions and follows the same empirical laws; but this remains true as long as one uses low-molecular weight surfactant like SDS and GCK (providing "fluid-like" interfaces). In such situations, for a given liquid fraction, we get $G'_L \approx \tau_y \approx R^{-1}$.

However, the chemical formulation can have an effect on the viscous and elastic moduli in the linear regime: we show that for the protein foams, with highly viscoelastic interfaces and gelified liquid films, one get lower G'_L and higher G''_L than with low molecular weight surfactants.

In addition, aging effects are clearly evidenced; some can be explained by the foam coarsening and drainage. But, the aging behavior of G''_L for low molecular weight surfactants like SDS is surprisingly the most anomalous and hard to explain as it does not fit with the foam aging itself.

The yield stress strongly decreases with the liquid fraction and follows the empirical law already observed for emulsions. For the yield stress, we have finally got limited differences between the surfactants and with the mode of measurements (continuous *vs* oscillatory).

Above the yield stress, the viscoelastic moduli plotted as a function of the strain follow a power law with close exponents, but different to those predicted by the most recent models;[19,20] they turn out to be more in agreement with the other experimental works and with the existence of a factor of 2 between the G' and G'' exponent.[28] We have shown here that these exponents in the non-linear regime depend on the liquid fraction and surfactant, and we have found that these exponent values obtained in oscillatory measurements are consistent with the measurements obtained by steady-shear experiments on the viscous stress.[9] This shows that oscillatory experiments above the yield strain, in the non-linear regime, have some physical meaning, correlated to steady shear conditions.

In this study, we have also provided experimental data obtained by a new oscillatory protocol (oscillations at constant shear rate). We have shown that this is a quite useful and novel approach. With this protocol, it becomes then possible to study usually inaccessible low frequency behaviors, simply by applying a constant shear rate. Under oscillations at constant shear rate, the curves of the moduli as a function of the frequency shows for the first time the occurrence of a characteristic frequency Ω_i. This frequency Ω_i depends on the shear rate with two regimes: one at low shear rates controlled by the coarsening, and a second controlled by the strain rate. A smooth crossover is observed between these shear-induced and coarsening-induced behaviors

We have shown for the first time that this macroscopic measurement of the characteristic frequency corresponds surprisingly well to the measurement of the rearrangement rate done by DWS (Fig.7): a direct link can then be drawn between a macroscopic and a microscopic measurement. This also explains the origin of the bump in the G'' data (either *versus* frequency or strain): in simple terms, it occurs when the intrinsic frequency (being a function of the shear rate) coincides to the experimental frequency. In that respect, it shows the importance of the shear rate, rather than the shear itself: scanning the sample in frequency *at constant strain* is not relevant. One must keep the *strain rate* constant to get the relevant information.

We have then evidenced that the non-linear regimes at low frequencies and at high deformations are identical for both G' and G'' (since $\delta \approx \delta'$, $\beta \approx \beta'$); in this regime, G'' becomes bigger than G' and the foam is then more fluid than elastic. Note also that we have found that the same value (slightly below 1) is found for the exponent ξ (dependence of Ω_i with the shear rate) as for δ and δ', and for the viscosity *vs* shear rate in steady-shear.

In fact, we have shown that we can compile all these similarities in the framework of a single solid-liquid transition: the transition is controlled by a nondimensional Deborah number, which represents both if the experimental frequency is either above or below the intrinsic frequency, and if the strain is either above or below a yield strain. The fact that, in the fluid-like regime ($De < 1$ implying $G'' > G'$), we have observed the same qualitative behavior for G' and G'' is due to the fact that—at the microscopic level—the unjamming of the foam is made by the same topological elementary rearrangements (T1), and that a coarsening-induced T1 and a shear-induced T1 are identical.

In a more general picture, we believe that this type of oscillatory measurements could help in testing if the microscopic

mechanisms linked to the slow relaxations occurring in many aging systems are identical to those obtained under shear.

As a last comment, looking back to the list of pending issues raised in the introduction and to the previous summary of results, it seems to us that this experimental work can have an important impact on the field by two ways. Firstly, we propose here a set of controlled data on the linear and non-linear regimes, on yielding, and on the effects of aging obtained on controlled samples. At this stage, there was a lack of such a catalogue of experimental data. On these issues, theoretical works are indeed more in advance and we believe that these results will then be useful for testing models, especially regarding the dependence with the chemical components and the liquid fraction. Secondly, this work confirms that oscillatory experiments done at constant shear rate are a powerful approach for studying soft materials and that the measurements of G' and G'' in the non linear regime are then meaningful. Here, for foams, we show that—once the experiments are performed following this protocol—we can reconcile some of the microscopic and macroscopic features, and that the characteristics of the fluid-like to solid-like crossover can be finally described by the use of the Deborah number.

References

1 R. Höhler and S. Cohen-Addad, *J. Phys.: Condens. Matter*, 2005, **17**, R1041.
2 H. M. Princen, in *Encyclopedia of Emulsion Technology*, ed. J. Sjöblom, Marcel Dekker, New York, 2001, p. 243.
3 H. M. Princen and A. D. Kiss, *J. Colloid Interface Sci.*, 1986, **112**, 427.
4 H. M. Princen and A. D. Kiss, *J. Colloid Interface Sci.*, 1989, **128**, 176.
5 S. A. Khan, C. A. Schnepper and R. C. Armstrong, *J. Rheol.*, 1988, **32**, 69.
6 A. Saint-Jalmes and D. J. Durian, *J. Rheol.*, 1999, **43**, 1411.
7 A. D. Gopal and D. J. Durian, *Phys. Rev. Lett.*, 2003, **91**, 188303.
8 N. D. Denkov, V. Subramanian, D. Gurovich and A. Lips, *Colloids Surf. A*, 2005, **263**, 129.
9 S. Marze, A. Saint-Jalmes and D. Langevin, *J. Rheol.*, 2008, **52**, 1091.
10 K. Golemanov, N. D. Denkov, S. Tcholakova, M. Vethamutu and A. Lips, *Langmuir*, 2008, **24**, 9956.
11 S. Tcholakova, N. D. Denkov, K. Golemanov, K. P. Ananthapadmanabhan and A. Lips, *Phys. Rev E*, 2008, **78**, 011405.
12 D. J. Durian, D. A. Weitz and D. J. Pine, *Phys. Rev. A*, 1991, **44**, R7902.
13 M. U. Vera, A. Saint-Jalmes and D. J. Durian, *Applied Optics*, 2001, **40**, 4210.
14 B. Dollet and F. Graner, *J. Fluid Mech.*, 2007, **585**, 181.
15 D. J. Durian, *Phys. Rev. E*, 1997, **55**, 1739.
16 Y. Wang, K. Krishnan and M. Dennin, *Phys. Rev. E*, 2006, **73**, 031401.
17 E. Janiaud, D. Weaire and S. Hutzler, *Phys. Rev. Lett.*, 2006, **97**, 038302.
18 S. Marze, A. Saint-Jalmes and D. Langevin, *Colloids Surf. A*, 2005, **263**, 121.
19 P. Marmottant and F. Graner, *Eur. Phys. J. E*, 2007, **23**, 337.
20 R. Höhler, S. Cohen-Addad and V. Labiausse, arXiv:cond-mat/0610279.
21 A. Saint-Jalmes, *Soft Matter*, 2006, **2**, 836.
22 A. Saint-Jalmes, M. U. Vera and D. J. Durian, *Eur. Phys. J. B*, 1999, **12**, 67.
23 K. Feitosa, S. Marze, A. Saint-Jalmes and D. J. Durian, *J. Phys.: Condens. Matter*, 2005, **17**, 6301.
24 V. Bergeron, *J. Phys.: Condens. Matter*, 1999, **11**, R215.
25 A. Saint-Jalmes, S. Marze, D. Langevin, in: *Food Colloids 2004: Interactions, Microstructure and Processing*, ed. E. Dickinson, Royal Society of Chemistry, Cambridge, 2004, p. 273.
26 B. V. Derjaguin, *Kolloid-Z*, 1933, **64**, 1.
27 A. J. Liu, S. Ramaswamy, T. G. Mason, H. Gang and D. A. Weitz, *Phys. Rev. Lett.*, 1996, **76**, 3017.
28 K. Miyazaki, H. M. Wyss, D. A. Weitz and D. R. Reichman, *Europhys. Lett.*, 2006, **75**, 915.
29 H. M. Wyss, K. Miyazaki, J. Mattsson, Z. Hu, D. Reichmann and D. A. Weitz, *Phys. Rev. Lett.*, 2007, **98**, 238303.
30 T. G. Mason, J. Bibette and D. A. Weitz, *Phys. Rev. Lett.*, 1995, **75**, 2051.
31 T. G. Mason, J. Bibette and D. A. Weitz, *J. Colloid Interface Sci.*, 1996, **179**, 439.
32 T. G. Mason, M. D. Lacasse, G. S. Grest, D. Levine, J. Bibette and D. A. Weitz, *Phys. Rev. E*, 1997, **56**, 3150.
33 D. Stamenovic, *J. Coll. Int. Sci.*, 1991, **145**, 255.
34 L. W. Schwartz and H. M. Princen, *J. Colloid Interface Sci.*, 1987, **118**, 201.
35 D. A. Reinelt and A. M. Kraynik, *J. Colloid Interface Sci.*, 1989, **132**, 491.
36 B. S. Gardiner, B. Z. Dlugogorski and G. J. Jameson, *J. Non-Newtonian Fluid Mech.*, 2000, **92**, 151.
37 R. Krishnaswamy, S. Majumbar and A. K. Stood, *Langmuir*, 2007, **23**, 12951.
38 A. D. Gopal and D. J. Durian, *J. Coll. Int. Sci.*, 1999, **213**, 169.
39 B. Abou and F. Gallet, *Phys. Rev. Lett.*, 2004, **93**, 160603-1.

This journal is © The Royal Society of Chemistry 2009